Characterization of Photonic Crystal Microcavities with Manufacture Imperfections

José M. Rico-García, José M. López-Alonso, and Javier Alda

Optics Department. University Complutense of Madrid.
School of Optics. Av. Arcos de Jalón s/n. 28037 Madrid. Spain.

jmrico@fis.ucm.es es; jmlopez@opt.ucm.es; j.alda@fis.ucm.es
http://www.ucm.es/info/aocg

Abstract:

The manufacture of a photonic crystal always produce deviations from the ideal case. In this paper we present a detailed analysis of the influence of the manufacture errors in the resulting electric field distribution of a photonic crystal microcavity. The electromagnetic field has been obtained from a FDTD algorithm. The results are studied by using the Principal Component Analysis method. This approach quantifies the influence of the error in the preservation of the spatial-temporal structure of electromagnetic modes of the ideal microcavity. The results show that the spatial structure of the excited mode is well preserved within the range of imperfection analyzed in the paper. The deviation from the ideal case has been described and quantitatively estimated.

© 2005 Optical Society of America
OCIS codes: (350.3950) Micro-optics, (230-3990) Microstructured devices, (000.5490) Probability theory, stochastic processes, and statistics

References and links

1. G. Guida, T. Brillat, A. Amouche, F. Gadot, A. De Lustrac, A. Priou "Dissociating the effect of different disturbances on the band gap of a two dimensional photonic crystal", J. App. Phys., **88**, 4491-4497, (2000).
2. N. A. Mortensen, M. D. Nielsen, J. R. Folkenberg, K. P. Hansen, J. Lgsgaard " Small-core photonic crystal fibers with weakly disordered air-hole claddings " J. Opt. A Pure Appl. Opt., **6**, 221-223, (2004)
3. M. Bayindir, E. Cubukcu, I. Bulu, T. Tut, E. Ozbay, C. Soukoulis. "Photonic band gaps, defect characteristics, and waveguiding in two-dimensional disordered dielectric and metallic photonic crystals " Phys. Rev. B, **64**, 195113-7, (2001)
4. G.Guida, "Numerical studies of disordered photonic crystals ", Progress in Electromagnetic Research (PIER), **41**, 107-131, (2003)
5. W. R. Frei, H. T. Johnson "Finite-element analysis of disorder effects in photonic crystals", Phys. Rev. B, **70**, 165116-11, (2004)
6. D. F. Morrison, *Multivariate Statistical Methods*, 3rd ed. (McGraw-Hill, Singapore, 1990) Chap. 8.
7. J. M. López-Alonso, J. Alda, E. Bernabéu, "Principal component characterization of noise for infrared images",Appl. Opt., **41**, 320-331, (2002).
8. J. M. López-Alonso, J. M. Rico-García, J. Alda, " Photonic crystal characterization by FDTD and principal component analysis", Opt. Express, **12**, 2176-2186, (2004).
9. S. Guo, S. Albin " Numerical Techniques for excitation and analysis of defect modes in photonic crystals" Opt. Express, **11**, 1080-1089 (2003).
10. J. M. López-Alonso, J. M. Rico-García, J. Alda, "Numerical artifacts in finite-difference time-domain algorithms analyzed by means of Principal Components", IEEE Trans. Ant. & Prop. (in press) (2005).

11. M. Skorobogatiy, G. Bégin, A. Talneau, "Statistical analysis of geometrical imperfections from the images of 2D photonic crystals", Opt. Express, **13**, 2487-2502, (2005).
12. M. Qiu, S. He "Numerical method for computing defect modes in two-dimensional photonic crystals with dielectric or metallic inclusions", Phys. Rev. B, **61**, 12871-12876, (2000).
13. P. R. Villeneuve, S. Fan, and J. D. Joannopoulos "Microcavities in photonic crystals: mode symmetry, tunability, and coupling efficiency", Phy. Rev. B, **54**, 7837-7842, (1996).
14. A. Taflove, S. Hagness, "Computacional Electrodynamics: The Finite-Difference Time Domain Method", 2nd edition, Artech House (2000).
15. J. M. López-Alonso, J. Alda, "Bad pixel identification by means of the principal component analysis", Opt. Eng., **41**, 2152-2157 (2002)
16. J. M. López-Alonso, J. Alda, "Characterization of artifacts in fully-digital image-acquisition systems. Application to web cameras", Opt. Eng., **43**, 257-265 (2004)

1 Introduction

Manufacture imperfections in real photonic crystal structures are unavoidable. In fact, the disorder provoked by them might be a drawback in the performance of any photonic device. Alterations in the high-simmetry structure of the crystal may lead to unexpected deviations from theoretical designs. Changes in the band-gap of filters and resonant cavities have been reported, both numerically and experimentally [1]. Modes of photonic crystal fibers are modified if a random perturbation is introduced into the fiber cladding [2]. Then, a simmetry-breaking mechanism drives a modification in the higher-order modes characteristics, whereas the fundamental mode remains unaffected. Crystals made of dielectrics materials show a different behaviour than their metallic counterparts under equal degree of disorder [3]. The reality is that a certain amount of disorder in a photonic crystal can be important, and the net effect in its working parameters could be noticeable. However, it is a tough task to get randomness into numerical computations[4]. Extensive simulations are required to achieve statistically meaningful results, regardless the method used to compute crystal parameters. Thus, the amount of data generated can be very large, and extracting useful information is challenging. Furthermore, a realistic simulation of manufacture errors involves structures that keep periodicy on the average, the so-called extended defect crystals [4]. Here, disorder stems from site displacements and size randomness of the fundamental units of the crystal [5].

The aim of this paper is to make use of a statistical multivariate technique, called Principal Component Analysis (PCA) [6, 7], to draw conclusions about the performance of a two-dimensional photonic crystal microcavity when a significative manufacture error is present. Although the paper studies a given geometry and structure, the proposed analysis can be applied to any other photonic crystal structure (microcavities, waveguides, couplers, etc.) in a similar manner. In a previous paper [8], PCA has successfully characterized the modes of a well-known photonic structure [9]. Also, the numerical noise embedded in FDTD simulations has been quantified and filtered using PCA [10].

The paper has been organized as follows. Section 2 presents the statistical and computational tools that we have used to carry out this analysis. In this section we have included a brief presentation of the physical constrains of the FDTD algorithm and the conditions of the excitation source. This is the same employed for the unperturbed, ideal, microcavity. In this section we have also included a brief summary of the PCA method. Section 3 contains the analysis of the results obtained from the numerical simulation. This analysis has been only possible when the PCA method is applied. The evolution of the electromagnetic field is calculated and related to the modes of the original structure by means of PCA. It is worthwhile to mention that this approach helps to know a priori the differences between the actual field and the theoretical prediction whether fabrications tolerances were provided [11]. Finally, section 4 summarizes the main conclusions of the paper.

2 Modelization and Simulation of the Perturbed Photonic Crystal

2.1 *Manufacture errors*

The photonic crystal analyzed in this paper is a microcavity showing defect modes within a near infrared bandgap [9]. The geometrical structure has been perturbed by allowing a controlled amount of change in the geometric parameters of the cylinders of the photonic crystal (see Figure 1). The values of the electric permittivity of the materials composing the microcavity (GaAs rods in air) remain unchanged. These cylinders are characterized by their location and their radii. For an ideal microcavity, all the cylinders are equal but the central one (the defect) which is larger than the rest of them. The cylinders are arranged in a regular rectangular grid. This geometry is perturbed to simulate the manufacture imperfections. In this paper the centers of the cylinders can be moved from their nominal position. The shape of the rods changes from a circular shape to a more general elliptic form. Then, each cylinder is characterized by five parameters: location of the center of the cylinder, p_x, p_y (along the x and y directions), values of the major and minor axis of the ellipse defining the cylinder, r_M, r_m, and orientation of the ellipse itself with respect to the reference frame, θ. The probability distribution functions that generate these five parameters for each rod have been Gaussian distributions for the dimensional parameters (location and axis of the ellipse), and an uniform distribution for the angular parameter. The Gaussian probability distribution function for each variable can be written as follows,

$$\mathrm{PDF}_Z = \frac{1}{\sigma_Z\sqrt{2\pi}} \exp\left[-\frac{(Z-\mu_Z)^2}{2\sigma_Z^2}\right], \tag{1}$$

where Z denotes one of the following variables or subindices, $Z = \{p_x, p_y, r_M, r_m\}$. The values used in this paper are defined as follows: $\mu_{p_x} = p_{x,N}$, and $\mu_{p_y} = p_{y,N}$, being $p_{x,N} = p_{y,N}$ the nominal values considered for the perfect microcavity (the pair of these nominal values characterizing the location of each cylinder are different); $\mu_{r_M} = \mu_{r_m} = r_N$, where r_N is the radius of the cylinders of the perfect case (all the cylinders have the same value but the central one); $\sigma_{p_x} = \sigma_{p_y} = a \times E$, where a is the lattice constant of the perfect crystal, and E is the manufacture error level; and $\sigma_{r_M} = \sigma_{r_m} = r_N \times E$. This level has been selected to have three values expressed as percentages: 1%, 3%, and 5% ($E = 0.01, 0.03$, and 0.05 respectively). The results recently obtained from the statistical analysis of images of fabricated photonic crystals show that the measured values of imperfection are within the range proposed in this paper [11]. The uniform distribution generating the orientation angle of the elliptical shape of each rod is defined within $[0, \pi)$. As we will see, this approach introduces an important increment in the information needed to describe a given realization of the photonic crystal. For an unperturbed microcavity we only need three parameters: radius of the cylinders of the grid, r_N; radius of the central cylinder, $r_{N,\mathrm{central}}$; and the spatial period of the crystal arranged in a squared grid, a. Now, each realization of the perturbed photonic crystal needs 125 parameters when an arrangement of 5×5 cylinders are considered. These previous probability distributions have been used to generate an ensemble of 100 realizations of the dielectric permittivity map. In Figure 1 we present the location and shape of the rods for three realizations having three different levels of manufacture errors (1%, 3%, and 5%, from left to right). In the case treated here, the nominal values are: $r_N = 0.2\mu$m, $r_{N,\mathrm{central}} = 0.6\mu$m, and $a = 1\mu$m. The white regions around the rods represent the locations of the rods along the 100 realizations studied in this paper. This white area increases with the manufacture error.

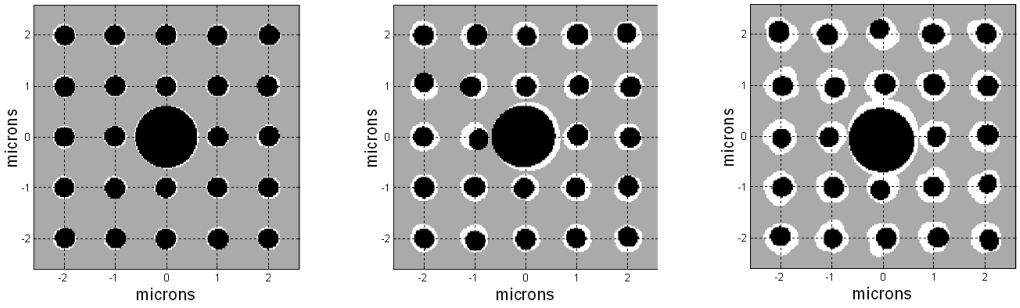

Fig. 1. Permittivity maps for three realizations of the photonic crystal microcavity. The error increases from left to right (1%, 3%, and 5%). The white portion around the rods represent the possible locations of the rods for the statistical realizations analyzed in this paper. This portion grows as the manufacture imperfection increases.

2.2 *The FDTD simulation*

As it has been explained elsewhere [12, 13], the photonic microcavity has a band-gap for TMz polarized fields (E_z,H_x,H_y components). Modes are produced because of the central cylinder defect (see figure 1). The band-gap encloses frequencies between 0.29 $\frac{c}{a}$ and 0.42 $\frac{c}{a}$ [9] (c is the speed of light). We look for spatial-temporal changes in the evolution of the modes when the dielectric structure is randomly perturbed. Hence, we supply the microcavity with energy in the same way as it is done when a mode of the original arrangement is excited. For the sake of simplicity, we have payed attention to the monopolar mode of the unperturbed crystal[9]. A "soft" [14] dipole source is placed in the center of the cavity. It evolves in time quasimonochromatically, oscillating at the original monopolar frequency[9]. The Maxwell equations are solved for TMz polarization in a 2D grid. The equations read as:

$$\partial_t H_x = -\frac{1}{\mu_0}\partial_y E_z \tag{2}$$

$$\partial_t H_y = \frac{1}{\mu_0}\partial_x E_z \tag{3}$$

$$\partial_t E_z = \frac{1}{\epsilon}(\partial_x H_y - \partial_y H_x) \tag{4}$$

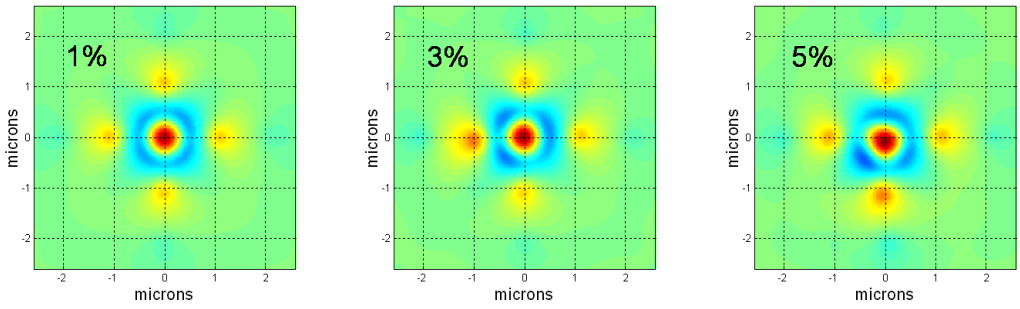

Fig. 2. Temporal evolution of the electric field component, E_z, for three realizations of the photonic crystal microcavity having manufacture errors (the realizations are the same than those presented in figure 1. The error increases from left to right: 1% (video file 1.78 Mb), 3% (video file 1.83 Mb), and 5% (video file 1.78 Mb). The unperturbed case can be seen in Fig. 7.c of reference [9].

The grid contains 221× 221 nodes. An Uniaxial Perfect Matched Layer[14] (UPML) surrounds the computational domain. It absorbs the outgoing waves running away from the photonic crystal. We have used a UPML having a thickness of 10 cells. The source is switched off after a convenient period of time. Then, the fields advance in time freely. The electric field is recorded over the whole grid each 10Δt, where Δt is the temporal step of the algorithm ($\Delta t = 5.886 \times 10^{-17}$). The spatial step, Δs, is 0.025 μm and the Courant factor is $S = 0.7063$. The field is recorded from $t_1 = 40000\Delta t$ to $t_2 = 41000\Delta t$ to form a sequence totaling 101 frames.

The electromagnetic fields are computed for each realization of the perturbed map of dielectric permittivity. Maxwell equations have been solved for the100 members of each ensemble to get a reliable PCA analysis. The output of the simulations are spatial-temporal maps of the electric and magnetic fields, resembling the monopolar mode of the unperturbed crystal. A complete simulation of an ensemble takes $\sim$ 7 hours in a Pentium 4 with 1 Gb of RAM memory and with a clock frequency of 2 GHz. The results of the FDTD algorithm for the realizations shown in Fig. 1 are presented in figure 2. The asymmetry of the mode clearly increases with the error.

2.3 *The PCA method*

The PCA method has been successfully used in a variety of fields where spatial-temporal set of data contains relevant pure spatial, pure temporal, and spatial-temporal mixed structures. This is the case of the characterization of noise in imaging devices, identification of bad pixels, extraction of spatial-temporal features in web cameras, both in the visible and the infrared [7, 15, 16]. We have also applied it to the analysis numeric artifacts appearing in FDTD results [8], in the characterization of a photonic crystal microcavity [10]. Although the basis of the method have been well established and fully developed in the referenced papers, we include a very short description of the characteristics of the method when applied to the analysis of FDTD frames. The key element of the method is the definition of statistical multidimensional variables realized a large amount of times. The multidimensional variable is the value of the electromagnetic field taken regularly in time (N times). Each point in the spatial grid corresponds with one statistical realization of the multidimensional variable. The next step is to define the covariance matrix among frames, S [7]. The diagonalization of this matrix produce three types of elements: eigenvalues, λ_k, eigenvectors, e_k, and eigenimages, PC_k, where k runs from 1 to N, being N the number of frames contained in the analyzed sequence. The eigenimages are also named as the principal components. They are uncorrelated among them and can be obtained as a rigid rotation from the original data. The coefficients describing the transformation between original data and principal components are given by the elements of the eigenvectors. The eigenvalues quantify the amount of variance associated with each principal component. A statistical analysis of the data allows the grouping of a collection of principal components into a single spatial-temporal structures that is named as process. This grouping diminishes the complexity of the original data and provide a straightforward method to filter undesirable contributions out from the original data. Each eigenvector describes the temporal evolution of the corresponding eigenimage. When the temporal evolution is quasi-harmonic, the identification of those eigenimages having a similar temporal evolution makes possible the definition of quasi-harmonic processes. All these facts where used in a previous contribution to characterize the presence of numerical noise, and some other artifacts, in the FDTD simulation of microcavities [8] [10]. The PCA method proved its validity to extract hidden spatial-temporal structures embedded in the original data and having interesting physical meanings. In this paper we have used the PCA method to analyze the sequence of frames obtained from the application of the FDTD to different realizations of a pho-

tonic crystal microcavity having manufacture errors. The results of the PCA are written as a collection of eigenvalues, $\lambda_k[j]$, eigenvectors, $e_k[j]$, and eigenimages, $\mathrm{PC}_k[j]$, where the subindex k denotes the order of the principal component and $[j]$ represents the given realization of the permittivity map.

3 Analysis and Results

PCA is applied after the fields have been calculated. Nevertheless, it should be noticed that we have excited the perturbed cavity as it if were unperturbed, because a real crystal works with the parameters provided by theoretical design studies, i.e., the parameters derived from the unperturbed crystal computation. Thus, if the manufacture tolerances can be estimated and introduced into the FDTD simulation, PCA puts into new light the statistical deviations from the expected performance and makes easier the analysis of the FDTD output. In this case, we are interested in the stability of the mode inside the cavity when the permittivity map does not correspond with the perfect photonic crystal.

In the case of the excitation of the monopolar mode of a perfect photonic crystal microcavity we found two quasi-monochromatic processes. Each one is composed of two electromagnetic distributions having the same temporal frequency and shifted $\pi/2$ in time one with respect to the other. They can be added to form a complex electromagnetic distribution. The first and second principal component have been identified with the real and imaginary part of a complex electromagnetic distribution corresponding with the monopolar mode (see [9] and [8]). The third and fourth principal components configure the second quasi-monochromatic process. We interpreted this second process as a standing wave having a temporal frequency outside the bandgap and surviving in the structure at a very low level (although its contribution explains only 0.013 % of the total variance of the data, the PCA method was able to show it and quantify its temporal evolution within the data). When the manufacture imperfections are included in the photonic crystal, the permittivity map losses its symmetry and periodicity. This will affect to the electromagnetic distribution within the microcavity for a given excitation. In our case, the excitation is not centered anymore. We saw that an almost negligible decentering of the excitation source in the case of the monopolar mode was able to excite some other modes, even in the perfect structure. Now, the perturbed photonic crystal is excited with a source located in the same place used to excite the monopolar mode in the perfect photonic crystal. As far as all the rods are allowed to move and deform within some given range, the centration is lost for every realization. Therefore, we expect the excitation of a variety of electromagnetic distributions within the structure, and not only those expected for the unperturbed crystal. The collection of basic electric field distributions in this paper has been taken from the PCA decomposition of the perfect photonic crystal excited with sources that generate the five modes described in reference [9]. We took the first four PCA for the monopolar excitation because we use the same excitation in the example shown in this paper. The first couple corresponds with the monopolar mode of the structure. For the other four excitations we only took the first two principal components (they describe the modes of the microcavity). Each couple forms a quasi-monochromatic process. The distribution of the electric field for the selected principal components are shown in Figure 3. All these electric field distributions will be used later to expand the results obtained from the PCA method.

The eigenvalues obtained from the PCA method, $\lambda_k[j]$, quantify the contribution to the total variance of the principal components in an ordinated manner. In the case treated here we are more interested in the description of the effect of a given amount of imperfection on the spatial-temporal evolution of the electric field. As far as the excitation corresponds with the monopolar mode, we expect that although the mode

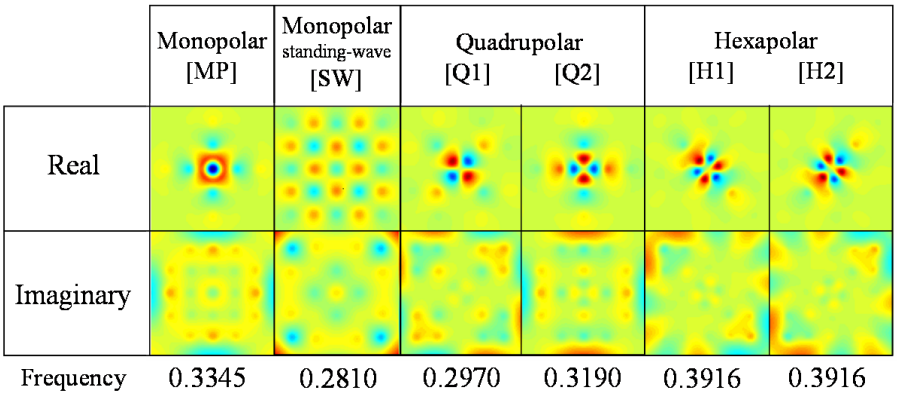

Fig. 3. Plot of the basic electric field distributions obtained from the PCA method for several excitations and for the unperturbed photonic crystal microcavity. The columns [MP] and [SW] are for the excitation of the monopolar mode. Only the column [MP] is describing the monopolar mode. These four plots are the first four eigenimages obtained from PCA (see figure 6). The columns [Q1] and [Q2] are the first two eigenimages for the two possible quadrupolar excitations. The columns [H1] and [H2] are for the hexapolar excitations. The eigenimages located in the same column correspond with eigenvalues having the same frequency but shifted $\pi/2$ in time. This temporal shift justifies their interpretation as Real and Imaginary parts of a complex mode (see reference [8]). The normalized frequency is shown below the column.

could be somehow deformed, the first eigenvalues will be related with the monopolar mode. In figure 4 we have represented the mean values of the eigenvalues, $\langle\lambda_k\rangle$, obtained after applying the PCA method to each FDTD sequence generated from each realization of the permittivity map ($\langle\rangle$ represents the ensemble average for all the $[j]$ realizations, $j = 1, \ldots, 100$). The error bars represent the 5% and 95% percentiles of the distribution of each eigenvalue. The three levels of manufacture imperfection are represented in different colors and slightly displaced horizontally for a better interpretation (this displacement will be repeated along the paper). The eigenvalue distribution obtained for the unperturbed photonic crystal has been plotted as a reference. We can see that only the first three eigenvalues are close to the case of the perfect microcavity. Even more, the disagreement grows as the level of imperfection increases. We can see that the first two eigenvalues are smaller than the eigenvalues obtained for the perfect case. However, the third and successive are larger than those belonging to the perfect microcavity. Besides, the rate of decreasing eigenvalue is slower as the imperfection grows. All this means that the variance of the data explained by the two first principal components, those expected to be associated with the unperturbed monopolar mode, decreases as the imperfections increases. This analysis is completed by computing the averaged relative contribution of the first two eigenvalues to the total variance of the data (see Table 1) . This contribution is calculated as $\langle\Omega_k\rangle = 100 \times \left\langle \frac{\lambda_k}{\sum_{k=1}^{N}\lambda_k} \right\rangle$ (N is the number of frames in the analyzed sequence). We may check that although the sum of the contributions of the first and second eigenvalues departs very slightly from the value obtained for the unperturbed microcavity (0% level of imperfection), the share between the first and the second changes: the second eigenvalue gains importance as the first eigenvalue contribution decreases.

The previous reasoning obtained from the eigenvalue evolution is reinforced by analyzing the spatial distribution of the electric field described by the first principal components averaged along the 100 realizations of the permittivity map, $\langle \mathrm{PC}_k \rangle$. These averages

Level of imperfection	$\langle\Omega_1\rangle$	$\langle\Omega_2\rangle$	$\langle\Omega_1\rangle + \langle\Omega_2\rangle$
0 %	99.059 %	0.929 %	99.987 %
1 %	99.06 %	0.93 %	99.99 %
3 %	98.60 %	1.26 %	99.85 %
5 %	96.64 %	2.67 %	99.32 %

Table 1. Relative contribution of λ_1 and λ_2 to the variance of the data

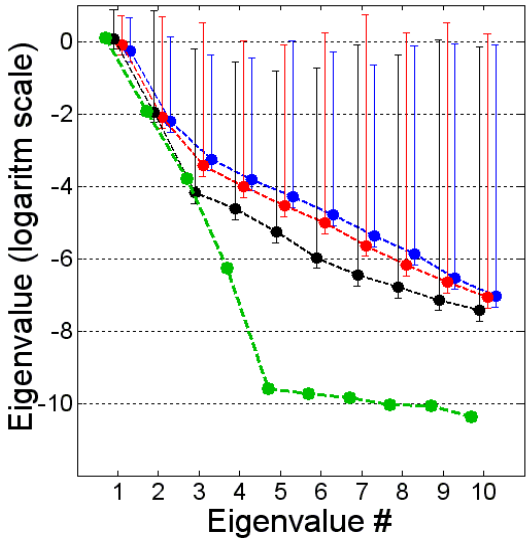

Fig. 4. Plot of the logarithm of the first ten eigenvalues obtained from the PCA decomposition. The unperturbed case (green) can be compared with the those cases showing a 1% (black), 3% (red), and 5% (blue) of error. The dots are for the ensemble average, $\langle\lambda_k\rangle$. The bars represent the range comprised within the 5% percentile and 95% percentile of the $\lambda_k[j]$ distribution. The horizontal location of the plotted points have been displaced to improve the representation.

are presented in Figure 5. It is clear that the first two averaged eigenvalues, $\langle \mathrm{PC}_1\rangle$, $\langle \mathrm{PC}_2\rangle$, are very close to those coming from the unperturbed microcavity. However, the third, and more clearly the fourth, are heavily perturbed with respect to the third eigenimage obtained for the unperturbed crystal. The deformation increases with the level of imperfection, as it should be expected. Even more, the averaged eigenimages somehow resemble the spatial patterns of modes of the photonic crystal microcavity mixed with the electric field distributions represented by the principal components obtained from the unperturbed crystal (see figure 3).

The previous analysis of the averaged principal components is complemented by presenting in figure 6 the spatial distribution of the first four principal components for the three realizations of the permittivity map at the three levels of imperfection presented in figure 1.

An important application of the PCA is the filtering of the data set by taking those principal components with a clear physical meaning. At the level of imperfection studied in this paper, only the first two principal components seem to be in good accordance with the expected results obtained for the unperturbed case. In figure 7 we have generated the spatial-temporal evolution of the filtered data using only the first two principal components. Besides, we have generated the evolution of the difference between the

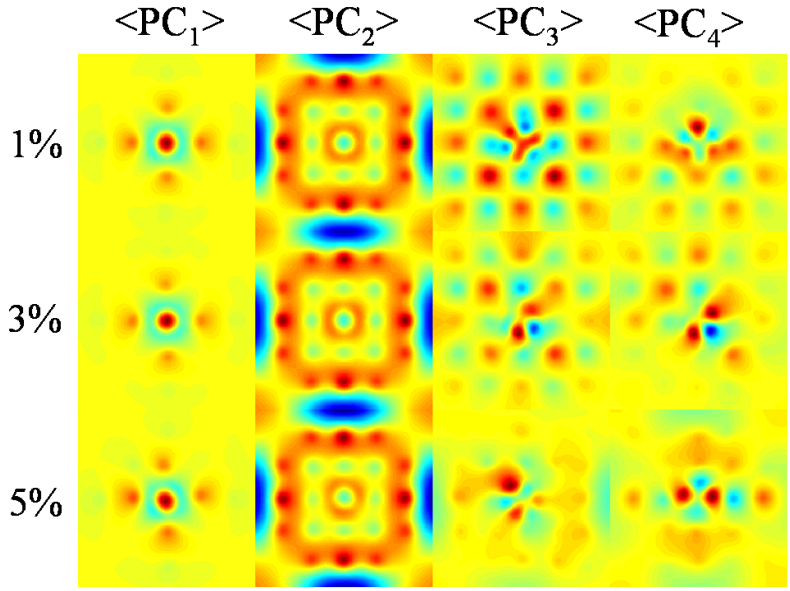

Fig. 5. Spatial distribution of the averaged principal components $\langle PC_1 \rangle, \langle PC_2 \rangle, \langle PC_3 \rangle$, and $\langle PC_4 \rangle$, for the three level of imperfection analyzed in this paper.

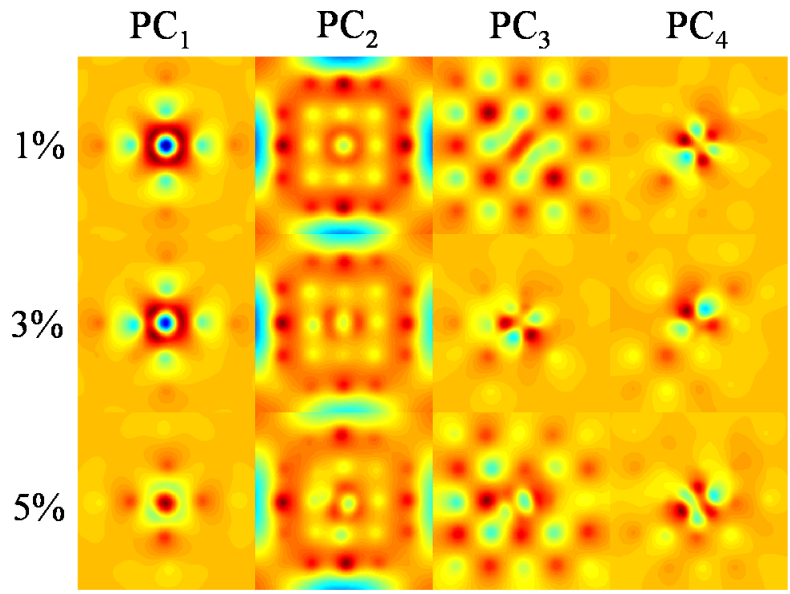

Fig. 6. Plot of the electromagnetic field distributions obtained from the first 4 principal components for three realization of the permittivity map (the same realizations presented in figures 1 and 2).

original and the filtered data for the selected realization (for the sake of simplicity we only show it for the case of 5% of imperfection). The filtered data resembles very much the shape of the monopolar mode. The evolution of the difference should be compared with the plot of Figure 4 of reference [8] where the same kind of filtering was applied to the results obtained for the unperturbed crystal.

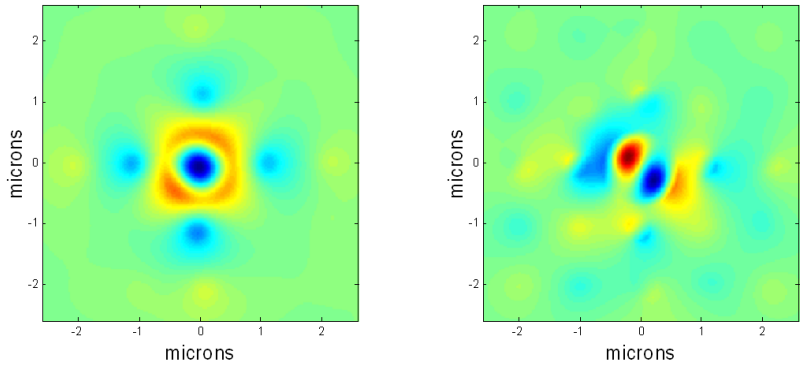

Fig. 7. On the left of this figure we present the spatial temporal evolution of the filtered version of the original data set at 5% level of imperfection (video file 1.09 Mb). The filtering has been performed by taking into account only the first two principal components. The difference between the original data and the filtered one is also presented for comparison on the right of the figure (video file 1.31Mb) . This difference takes into account only 1.9 % of the variance of the data set.

From the results obtained through the PCA we have performed another analysis of the data. In this case we have been interested in the description of the principal components in terms of the principal components produced by those excitations that generate the modes of the unperturbed microcavity applied to the perfect photonic crystal. These principal components were presented in figure 3. These electric field distributions are orthogonal and constitute a suitable non-complete base for the expansion of the results obtained for the actual realizations of the photonic crystal. The decomposition can be written as follows

$$\mathrm{PC}_k[j] = \sum_m \alpha_{k,m}[j] E_m + O_k[j], \tag{5}$$

where α_m is the coefficient of the decomposition, and E_m represents the normalized distribution of electric field obtained from the application of the PCA to the unperturbed photonic crystal. In our case, the chosen electric field distributions ,E_m, are real and have been represented in figure 3. The element $O_k[j]$ appearing in the previous equation denotes the part of the principal component, $\mathrm{PC}_k[j]$, that can not be expanded in the proposed base of functions. The calculation of these coefficients is given by

$$\alpha_{k,m}[j] = \iint \mathrm{PC}_k[j](x,y) E_m(x,y) dxdy. \tag{6}$$

In Table 2 we have evaluated the average for all the realizations of the percentage of energy of the principal component that is not described by the proposed non-complete base. We are assuming that each principal component is representing a real electric field distribution having an energy given as $\iint |\mathrm{PC}_k[j](x,y)|^2 dxdy$.

The results of this decomposition is shown in Figure 8. The plots on the left of the figure are for the absolute value of the $\langle |\alpha_{k,m}| \rangle$ coefficients for $k = 1, 2$, and 3, and m corresponding to the electric field distribution of figure 3 denoted as Re[MP], Im[M], Re[SW], Im[SW], Re[Q1], Re[Q2], Im[Q2], Re[H1] and Re[H2] (Re[] and Im[]

Level of imperfection	PC_1	PC_2	PC_3
1 %	0.32 %	0.25 %	4.71%
3 %	2.69 %	2.20 %	9.36 %
5 %	6.32 %	6.29 %	15.71 %

Table 2. Ensemble average of the percentage of energy explained by O_k, i. e., that is not described by the proposed non-complete base. The values are for the three first principal components and the three levels of imperfections analyzed in this paper.

denote the real and imaginary part of the complex electric field distribution of the quasi-monochromatic process). The coefficients for the remaining Im[Q1], Im[H1], and Im[H2] are negligible for the data considered in these plots. The error bars represent the standard deviation of the plotted data. In the right of this figure we have plotted $\langle|\cos\gamma_{k,m}|\rangle$. They are the ensemble average of the absolute value of the cosine of the angle between the given principal component and E_m. These cosines have been evaluated as

$$\cos\gamma_{k,m}[j] = \frac{\iint \mathrm{PC}_k[j](x,y)E_m(x,y)dxdy}{\sqrt{\iint |\mathrm{PC}_k[j](x,y)|^2\,dxdy}\sqrt{\iint |E_m(x,y)|^2\,dxdy}}. \tag{7}$$

The results for the first two principal components reinforce those obtained from the previous analysis of the principal components and eigenvalues. Both the first and the second principal components are mainly projected onto the Re[MP] and Im[MP] obtained from the unperturbed microcavity, as it should be expected. The projections of $PC_1[j]$ and $PC_2[j]$ on Re[MP] and Im[MP] respectively are larger, in average, for a lower level of manufacture error. For the third principal principal component, $PC_3[j]$, things are a little more complicated. For the lowest level of imperfection (1%) the projection on the Re[SW] spatial distribution is the largest. However, for the other two levels of manufacture errors, $PC_3[j]$, contains a non-negligible portion of the Hexapolar modes (Re[H1], and Re[H2]). This fact can be interpreted following the same reasoning used to justify the appearance of hexapolar modes when some decentration of the excitation source is allowed.[8] Another interesting appearance is the non-negligible contribution of the quadrupolar mode (labeled as Q2). The associated spatial distribution, Re[Q2], appears even in the first principal component, and it is more noticeable for a larger imperfection level. The justification of this result can be made taking into account the frequency of the mode. Although the excitation source is not adjusted for the generation of this mode, its frequency is the closest one to the temporal frequency of the excitation. Therefore, the transfer of energy to this mode should be easier than for the rest of the modes. It is important to note that this analysis can be applied to any realization of the photonic crystal, and the results can be interpreted for a given fabricated structure once its particular geometry is included in the simulation. In this sense, the proposed method can be also applied as "a posteriori" tool to evaluate the actual behavior of the electromagnetic field in terms of the electric field distributions expected for a perfect structure.

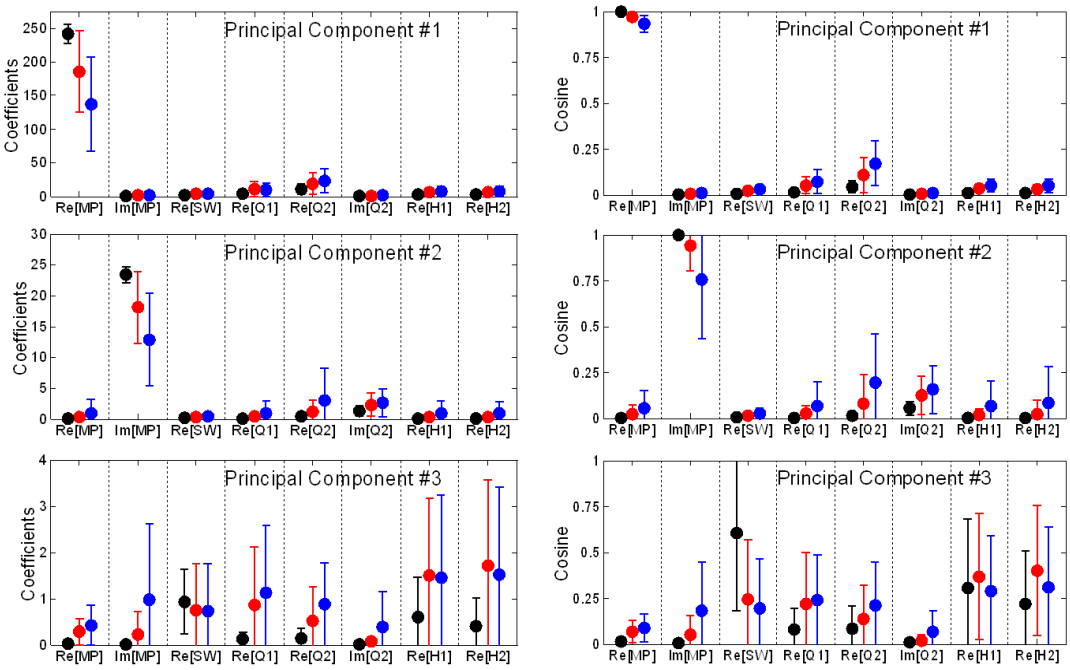

Fig. 8. Plots of the average and standard deviation (error bars) of the coefficients (left column) and cosines (right column) obtained when projecting the first three principal components on the basis of electromagnetic distributions obtained from the PCA method applied to the unperturbed photonic crystal . The labels on the horizontal axis denote the modes presented in Fig. 3. The three manufacture imperfections are presented with different colors 1% (black), 3% (red), and 5% (blue).

4 Conclusion

In this paper we have modeled the manufacture errors in the geometry of the elements of a photonic crystal microcavity formed by dielectric rods immersed in vacuum and having a central defect. A collection of permittivity maps have been generated using several probability distribution functions for the location and shape of the rods. The rods are allowed to be elliptic. The level of imperfection is included in the variance of the Gaussian probability distributions used to model the dimensional parameters. We have analyzed three levels of error with respect to the nominal value: 1%, 3% and 5%. For each error we have generated 100 photonic crystal microcavities. Each statistical realization has been excited with the same source. The characteristics and location of the excitation is the same used to generate the so-called monopolar mode in the ideal photonic crystal. The response of the crystal has been analyzed using an FDTD algorithm. A sequence containing 101 frames was recorded for each realization. Each one of the sequences has been analyzed using the PCA method. Although the analysis shown here is applied to a very specific case, we should recall that the method outlined in this paper can be extended to any other permittivity map, by defining the appropriate probability distribution functions and analyzing the FDTD results by using the PCA method.

The analysis of the eigenvalues obtained from the PCA for each permittivity map has shown that, within the range of manufacture error presented in this paper, the expected mode surviving in the microcavity is deformed in shape, but still explains most of the variance of the data, i. e., it contains most of the energy of the generated electric field. The amount of variance not related with the real part of the monopolar mode increases with the error level, reaching a mean value of 3.64% for the maximum level of error (5%). The dispersion of the eigenvalue distribution shows a large variability among statistical realizations. This variability is strongly reduced when considering the relative contribution of the eigenvalues to the total variance of the data. In this case, the results show a growing dispersion of values of these contributions when the error increases. All these results mean that the electric field is better explained not only taken into account the electric field distributions expected for the unperturbed crystal, but also considering some other electric field distributions within the microcavity.

An useful capability of the PCA is exploited in this paper when filtering the FDTD sequence obtained for a given realization of the permittivity map. The results show the filtered data resembling the expected monopolar mode. The difference between the original data and the filtered set contains spatial-temporal evolutions that can be related with some other electric field distributions within the crystal. In order to explain better the presence and origin of these electric field distribution we have built up a non-complete orthogonal base. The elements of this non-complete base are obtained from the PCA applied to the FDTD sequences obtained for the perfect photonic crystal excited with sources that generate the five defect modes in the bandgap of the structure. The principal components obtained for each realization has been expanded in this base. The analysis of the coefficients and projections of this expansion shows again that the main contributor to the evolution of the electric field is the expected monopolar mode. However, some other modes appear. The hexapolar modes seems to be generated by the lack of symmetry of the crystal, resembling the results obtained for the perfect microcavity excited with a slightly decentered source. Besides, the quadrupolar mode having its frequency the closest to the monopolar mode frequency is the one presenting the largest contribution. This means, that some of the energy fed into the cavity is transferred to this mode because of its closeness in frequency.

As a final remark, we should emphasize that the results shown here are only possible

when analyzing the FDTD data by using the PCA method. Although the method is blind in nature, it is able to extract enough information to justify and conclude important relations using the knowledge of the nature of the analyzed problem.

Acknowlegments

This work has been partially supported by the project TIC2001-1259 of the Ministerio de Ciencia of Tecnología of Spain, and by the project GR/MAT/0497/2004 of the Comunidad of Madrid, Spain.